



Supra- and infra-tentorial degeneration patterns in primary lateral sclerosis: a multimodal longitudinal neuroradiology study

Jana Kleinerova¹ · Marlene Tahedl¹ · Ee Ling Tan¹ · Siobhan Delaney^{1,2} · Jennifer C. Hengeveld³ · Mark A. Doherty³ · Russell L. McLaughlin³ · Orla Hardiman¹ · Kai Ming Chang¹ · Eoin Finegan¹ · Peter Bede^{1,2}

Received: 21 December 2023 / Revised: 14 February 2024 / Accepted: 15 February 2024 / Published online: 5 March 2024
© The Author(s) 2024

Abstract

Background Primary lateral sclerosis (PLS) is traditionally solely associated with progressive upper motor neuron dysfunction manifesting in limb spasticity, gait impairment, bulbar symptoms and pseudobulbar affect. Recent studies have described frontotemporal dysfunction in some patients resulting in cognitive manifestations. Cerebellar pathology is much less well characterised despite sporadic reports of cerebellar disease.

Methods A multi-timepoint, longitudinal neuroimaging study was conducted to characterise the evolution of both intra-cerebellar disease burden and cerebro-cerebellar connectivity. The volumes of deep cerebellar nuclei, cerebellar cortical volumes, cerebro-cerebellar structural and functional connectivity were assessed longitudinally in a cohort of 43 individuals with PLS.

Results Cerebello-frontal, -temporal, -parietal, -occipital and cerebello-thalamic structural disconnection was detected at baseline based on radial diffusivity (RD) and cerebello-frontal decoupling was also evident based on fractional anisotropy (FA) alterations. Functional connectivity changes were also detected in cerebello-frontal, parietal and occipital projections. Volume reductions were identified in the vermis, anterior lobe, posterior lobe, and crura. Among the deep cerebellar nuclei, the dorsal dentate was atrophic. Longitudinal follow-up did not capture statistically significant progressive changes. Significant primary motor cortex atrophy and inter-hemispheric transcallosal degeneration were also captured.

Conclusions PLS is not only associated with upper motor neuron dysfunction, but cerebellar cortical volume loss and deep cerebellar nuclear atrophy can also be readily detected. In addition to intra-cerebellar disease burden, cerebro-cerebellar connectivity alterations also take place. Our data add to the evolving evidence of widespread neurodegeneration in PLS beyond the primary motor regions. Cerebellar dysfunction in PLS is likely to exacerbate bulbar, gait and dexterity impairment and contribute to pseudobulbar affect.

Keywords Primary Lateral Sclerosis · Cerebellum · Connectivity · Pharmaceutical trials · MRI

Abbreviations

AAL	Automated Anatomical Labeling (AAL) atlas
AD	Alzheimer's disease
ALS	Amyotrophic lateral sclerosis
ALSod	ALS online database
ANOVA	Analysis of variance (ANOVA)
ASO	Antisense oligonucleotide
BOLD	Blood-oxygen-level-dependent (BOLD) signal
C9+	ALS patients with GGGGCC hexanucleotide repeat expansion in C9orf72
C9-	ALS patients without GGGGCC hexanucleotide repeat expansion in C9orf72
C9orf72	Chromosome 9 open reading frame 72

Jana Kleinerova and Marlene Tahedl have contributed equally as joint first-authors.

✉ Peter Bede
bedep@tcd.ie

¹ Computational Neuroimaging Group (CNG), School of Medicine, Trinity College Dublin, Dublin 2, Ireland

² Department of Neurology, St James's Hospital, Dublin, Ireland

³ Smurfit Institute of Genetics, Trinity College Dublin, Dublin, Ireland

CC	Corpus callosum	PD	Parkinson's disease
CNS-LS	Center for Neurological Study- Liability Scale	PMC	Primary motor cortex
CSD	Constrained spherical deconvolution	PUMNS	Penn Upper Motor Neuron Score
CST	Corticospinal tract	QC	Quality control
CT	Cortical thickness	RH	Right hemisphere
DOFs	Degrees of freedom	Rt	Right
dMRI	Diffusion magnetic resonance imaging	RD	Radial diffusivity
ECAS	Edinburgh Cognitive and Behavioural ALS Screen	ROI	Region of interest
ELQ	Emotional Liability Questionnaire	rs-fMRI	Resting-state functional MRI
EMG	Electromyography	SC	Structural connectivity
EMM	Estimated marginal mean	SD	Standard deviation
EPI	Echo-planar imaging	SE-EPI	Spin echo planar imaging
FA	Fractional anisotropy	SENSE	Sensitivity Encoding
FC	Functional connectivity	SPIR	Spectral presaturation with inversion recovery
fMRI	Functional MRI	T	Tesla
FLAIR	Fluid-attenuated inversion recovery	T1w	T1-weighted imaging
fODF	Fibre orientation distribution function	TCV	Total cerebellar volume
FOV	Field of view	TDI	Track Density Imaging
FrSBe	Frontal Systems Behavior Scale	TE	Echo time
FSL	FMRIB's Software Library	TI	Inversion time
FTD	Frontotemporal dementia	TIV	Total intracranial volume
FTLD	Frontotemporal lobar degeneration	Tukey HSD	Tukey's Honest Significant Difference
FWE	Familywise error	TR	Repetition time
GM	Gray matter	UMN	Upper motor neuron
HADS	Hospital Anxiety and Depression Scale	VR	Voxel resolution
HARDI	High Angular Resolution Diffusion Imaging	WM	White matter
HC	Healthy control		
HD	Huntington's disease		
ICA-AROMA	Automatic Removal Of Motion Artifacts		
IR-SPGR	Inversion recovery prepared spoiled gradient recalled echo		
IQR	Interquartile range		
LAS	Local Adaptive Segmentation		
LH	Left hemisphere		
Lt	Left		
LMN	Lower motor neuron		
M1	Primary motor cortex		
ML	Machine-learning		
MND	Motor neuron disease		
MNI	Montreal Neurological Institute		
MNI152	Montreal Neurological Institute 152 standard space		
MRI	Magnetic resonance imaging		
MRS	MR spectroscopy		
NISALS	Neuroimaging Society in ALS		
NIV	Non-invasive ventilation		
NODDI	Neurite orientation dispersion and density imaging		
PBA	Pseudobulbar affect		
PCR	Polymerase chain reaction		

Introduction

PLS has traditionally been exclusively associated with primary motor cortex, corpus callosum and descending corticospinal tract degeneration [1–4], but there is a scarcity of longitudinal studies in PLS. [5–7]. There is however growing evidence of frontotemporal disease burden and supporting clinical evidence of frontotemporal dysfunction [8–12]. More recently, considerable subcortical disease burden has also been described, and putative extrapyramidal and cognitive correlates proposed [13–15]. There is a particularly high incidence of pseudobulbar affect in PLS, which is classically linked to cortico-bulbar disconnection [16, 17], but the contribution of impaired cerebellar gating is increasingly recognised as an important aetiological factor [18–23]. As PLS carries a considerably better prognosis than ALS [24], it is often inaccurately regarded as a relatively benign condition. However, recent research has helped to reconceptualise PLS from a pure UMN condition with a relatively benign course, to a relentlessly progressive neurodegenerative condition [25] with considerable extra-motor, frontotemporal, subcortical and cerebellar involvement. Despite landmark histopathology papers

[26], the post-mortem literature on PLS is relatively scarce, therefore quantitative imaging approaches are the most reliable techniques to characterise and track progressive disease burden trajectories. Both PET and MRI studies have contributed considerable insights, but the majority of imaging studies are cross-sectional. Previous diagnostic criteria required a minimum symptom duration of 4 years, which led to the inclusion of patients with considerable disease durations into research studies. The new consensus diagnostic criteria [27] and the introduction of the category “probable” PLS have enabled earlier recruitment and enrolment into academic research studies [28]. The characterisation of cerebellar pathology is a relatively novel frontier of PLS research, particularly in view of conflicting histopathology reports and the difficulty to appreciate clinical correlates of cerebellar disease. Cerebellar manifestations are likely to be masked by the predominant upper motor neuron signs and admittedly formal cerebellar assessments are not commonly performed in PLS. Some post-mortem reports described the cerebellum as ‘unremarkable’ [29] despite radiological reports of cerebellar involvement [9, 30, 31]. Global cerebellar volume loss is sometimes reported, but the predilection for specific cerebellar lobules is less well evaluated [32]. Recent quantitative imaging studies confirmed functional [33, 34] and structural cerebro-cerebellar connectivity changes [33, 34] and spinocerebellar tract degeneration have also been recently reported. [35] Considerable brainstem atrophy has also been shown in PLS, based on high-resolution structural data, which may be exacerbated by the degeneration of cerebellar projections. [36, 37] Notwithstanding the radiological evidence, overt cerebellar ataxia is not commonly noted clinically observed in PLS. [34, 35, 38]. Cerebellar pathology in ALS is better characterised [39], in no small part due to the interest in *ATXN1* and *ATXN2* repeat expansions, and genotype-associated cerebellar signatures have been proposed [40]. Evidence from other neurodegenerative conditions suggests that cerebellar pathology is likely to contribute to bulbar, eye-movement, gait, dexterity, cognitive, behavioural, pseudobulbar and respiratory manifestations in PLS also [38, 41–48]. Analogous to ALS [49–51], language deficits, behavioural impairment, deficits in social cognition and executive dysfunction have also been reported in PLS [8–12]. In view of recent imaging and clinical reports, our objective was the systematic characterisation of both intra-cerebellar and cerebro-cerebellar connectivity alterations in a large cohort of individuals with PLS and track integrity measures longitudinally over four timepoints.

Methods

Ethics approval

This project was approved by the Ethics Committee of Beaumont Hospital Dublin (REC reference: 08/90) and each participant gave informed consent prior to study enrolment.

Demographic, clinical and genetic profiling

A total of 156 participants, 43 PLS patients and 113 healthy controls (HC) were included in this study. Up to four MRI scans were acquired with a follow-up interval of four months. Demographic variables were carefully recorded; age, sex, symptom duration, handedness, education, and family history of neurodegenerative conditions (Table 1). Forty out of 43 patients had their total ALSFRS-r, ALSFRS sub-scores, symptom duration, Penn Upper Motor Neuron Score (PUMNS), modified Ashworth spasticity scale scores, Edinburgh Cognitive and Behavioural ALS Screen (ECAS), the Frontal Systems Behavior Scale (FrSBe), the Hospital Anxiety and Depression Scale (HADS), the Emotional Lability Questionnaire (ELQ) and the Center for Neurological Study-Lability Scale (CNS-LS) scores also recorded. A standardised cerebellar assessment was also performed on 31 patients by the same neurologist. Individuals with PLS were diagnosed based on the new consensus criteria [27]. Exclusion criteria for each participant included prior stroke, brain or neurovascular surgery, traumatic brain injury, and comorbid neurological or psychiatric diagnoses. Thirty-one of the 43 PLS patients underwent whole genome sequencing as described previously [52] and were screened for ALS [53] and HSP-associated [54] genetic variants. Thirty-three PLS were screened for *C9orf72* GGGGCC repeat expansions using repeat-primed polymerase chain reaction (PCR). GeneMapper version 4.0 was used to visualise capillary electrophoresis outcomes more than 30 repeats were considered *C9orf72*-positive.

Neuroimaging

A standardised neuroimaging protocol was implemented on a 3 Tesla Philips Achieva MR scanner. The protocol included T1-weighted (T1w), fluid-attenuated inversion recovery (FLAIR), diffusion-MRI (dMRI), resting state functional MRI (rs-fMRI) sequences. A 3D Inversion Recovery prepared Spoiled Gradient Recalled echo (IR-SPGR) sequence was implemented to acquire T1w images with: TR / TE = 8.5/3.9 ms, TI = 1060 ms, FOV of 256 × 256 × 160 mm, 160 sagittal slices with no interslice gap, flip angle (FA) = 8°, VR = 1 mm³, SENSE factor = 1.5. An Inversion

Table 1 Demographic details of the study population

	PLS	HC	PLS vs HC t-test ⁺ / Chi-square test ⁺⁺
Number of subjects at baseline (T1/dMRI/rs-fMRI)	43 (43/41/39)	113 (113/113/111)	<i>n.a.</i>
Number of subjects at Time-point 2 (T1/ dMRI/rs-fMRI)	8 (30/29/27)	18 (18/18/18)	<i>n.a.</i>
Number of subjects at Time-point 3 (T1/ dMRI/rs-fMRI)	7 (25/25/23)	13 (13/13/13)	<i>n.a.</i>
Number of subjects at Time-point 4 (T1/ dMRI/rs-fMRI)	3 (20/19/15)	8 (8/8/8)	<i>n.a.</i>
Age [y, mean ± SD]	55.50 ± 9.05	59.36 ± 10.66	$t(80.33) = 1.33$, $p = .188$
Years of education [y, mean ± SD]	12.18 ± 3.25	14.77 ± 3.46	$t(71.04) = -4.05$, $p = .001^*$
Sex, F/M	16/27	57/56	$\chi^2(1, N = 156) = 1.69$, $p = .193$
Handedness, R/L	39/4	106/7	$\chi^2(1, N = 156) = 0.11$, $p = .736$
Years of symptom duration [y, mean ± SD]	109.75 ± 70.46	<i>n.a.</i>	<i>n.a.</i>

[#]Follow-up scans were acquired with an inter-scan interval of four months

dMRI diffusion-weighted imaging, *F* female, *rs-fMRI* resting-state functional MRI, *HC* healthy control, *L* left-handed, *M* male, *MRI* magnetic resonance imaging, *n.a.* not applicable / not available, *PLS* primary lateral sclerosis, *R* right-handed, *SD* standard deviation, *y* years

⁺Welch two-sample t-tests [*t*] were performed to test differences of age and years of education between all PLS vs. HC

⁺⁺Chi-square tests [χ^2] were performed to test differences of sex and handedness frequencies between all PLS patients vs. HC

*significant at an alpha-level of $p \leq 0.05$

Recovery Turbo Spin Echo (IR-TSE) sequence was utilised to acquire FLAIR images axially with a repetition time (TR) / echo time (TE) = 11,000/125 ms, inversion time (TI) = 2800 ms, field of view (FOV) = 230 × 183 × 150 mm, voxel resolution (VR) = 0.65 × 0.87 × 4 mm. A spin-echo echo planar imaging (SE-EPI) pulse-sequence was used to record dMRI data with a 32-direction Stejskal-Tanner diffusion encoding scheme: TR/TE = 7639/59 ms, FOV = 245 × 245 × 150 mm, 60 axial slices with no interslice gaps, FA = 90°, VR = 2.5 mm³, SENSE factor = 2.5, dynamic stabilisation and spectral presaturation with inversion recovery (SPIR) fat suppression. An echo-planar imaging (EPI) sequence was used to acquire 220 volumes of rs-fMRI data to assess blood oxygen level-dependent (BOLD) signal at rest with TR/TE = 2000/35 ms, FOV = 233 × 233 × 120 mm, 30 axial slices with no interslice gap, FA = 90°, VR = 2.875 mm × 2.875 mm × 4 mm, SENSE factor = 2.5. Participants were instructed to close their eyes during the rs-fMRI data acquisition.

Structural analyses

The Computational Anatomy Toolbox (CAT12) [55] was implemented to assess cerebellar grey matter (GM) alterations. Pre-processing steps included denoising, affine registration, partial volume segmentation, skull-stripping and spatial normalization. Cerebellar cortical regions-of-interest (ROIs) were defined using the SUIT cerebellar segmentation pipeline [56]: (1) anterior lobe (SUIT labels I-V), (2) posterior lobe (SUIT labels VI-IX), (3) flocculonodular

lobe (SUIT) label X, (4) crura (SUIT labels “Crura I” and “Crura II”), and (5) vermis (SUIT labels “Vermis”). The Julich-Brain Cytoarchitectonic Atlas was used to define the cerebellar nuclei [57]: (1) dorsal dentate, (2), ventral dentate, (3) interposed, and (4) fastigial. The primary motor cortex (M1) was defined based on the labels “Brodmann 4a” labels from the Anatomy3 atlas [58]. GM volume of these ROIs were estimated separately in the two hemispheres using CAT12 and added to generate a single volume output for each ROI. *MRtrix3* was utilised for dMRI data pre-processing [59], which included denoising, Gibb’s Ringing artifact removal, motion-, eddy current- and bias field-corrections. Subsequent to dMRI data preprocessing, the constrained spherical deconvolution (CSD) approach was implemented [60] to estimate fibre orientation distribution (fODF) in each voxel before normalisation [61]. Tractography of the following tracts was performed: (1) cerebello-frontal, (2) cerebello-parietal, (3) cerebello-temporal, (4), cerebello-occipital, (5) cerebello-thalamic and (6) spinocerebellar i.e. inferior brainstem-cerebellum. Relevant masks were defined using SUIT, Automated Anatomical Labeling (AAL) atlas and Hammers atlas labels [62]. The corticospinal tract was mapped from the primary motor cortex to the brainstem in each hemisphere separately and transcallosal fibres were mapped between the right to left motor cortex. Probabilistic tractography [63] was performed with 5000 streamlines and the Track Density Imaging (TDI) approach was implemented [64] (Fig. 1). Two white matter integrity metrics, fractional

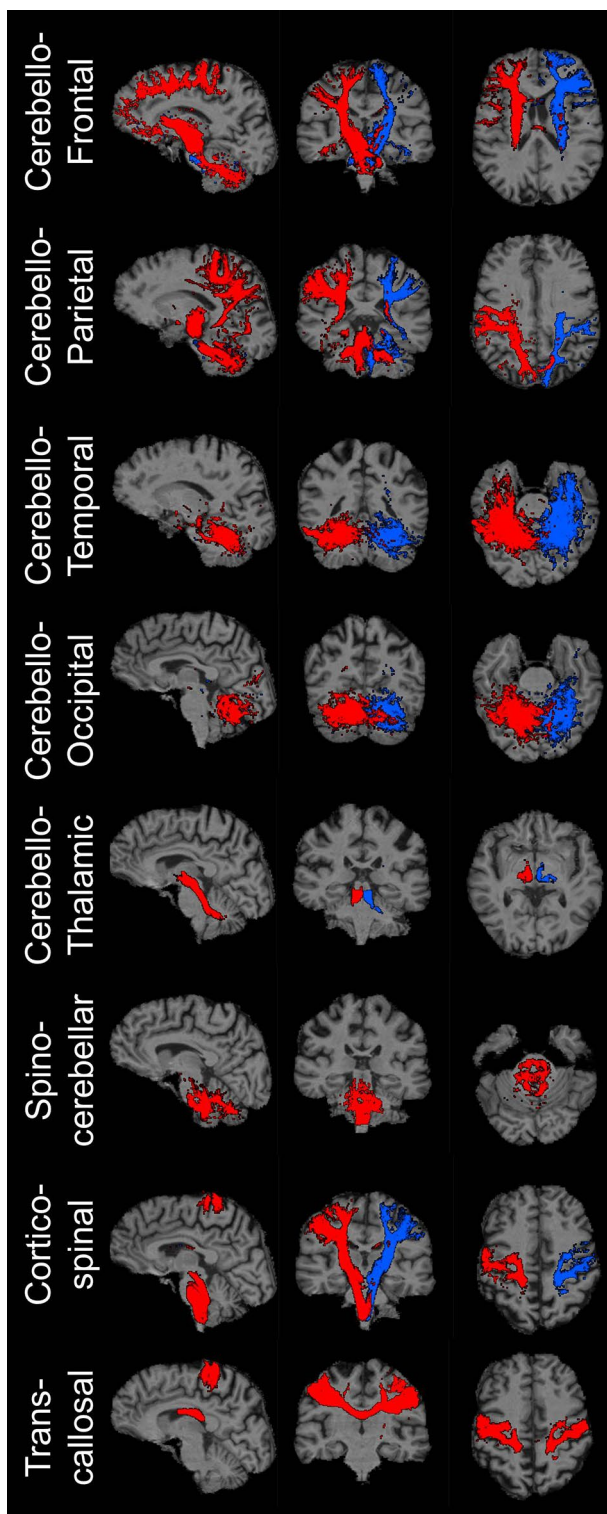


Fig. 1 Illustrative tractography outputs from a healthy control. Right-hemispheric and unilateral tracts are depicted in red, left-hemispheric tracts in blue

anisotropy (FA) and radial diffusivity (RD) were evaluated for each tract.

Functional analyses

BOLD signal correlations were explored between the above ROIs, along the CST and CC. The FEAT pipeline of the FMRIB Software Library (FSL) [65] was used to pre-process fMRI data including brain extraction, intensity normalisation, and slice-time corrections. FSL's ICA-based Automatic Removal Of Motion Artifacts (ICA-AROMA) [66] was utilised to correct for head-motion artifacts. Data were registered to MNI152 2mm standard space. As above, (1) cerebello-frontal, (2) cerebello-parietal, (3) cerebello-temporal, (4), cerebello-occipital, (5) cerebello-thalamic and (6) cerebello-spinal functional connectivity were appraised. Fisher z -transformed Pearson correlations were run between the mean BOLD time courses of the above pairs of ROIs in Matlab R2022b (The Mathworks, Natick, USA) using the CoSMoMVPA [67] toolbox.

Statistical modelling

Statistical analyses were performed with RStudio (version 2022.12.0 + 353; R version 4.2.2).

Differences in means of age and education between PLS patients and HC were investigated using Welch two-sample t -tests, whereas differences in sex and handedness frequencies were compared using Chi-square testing. To test for cross-sectional differences in neuroimaging metrics between PLS patients and HC, we implemented a one-way analysis of variance (ANOVA), correcting for the confounding effects of age, sex, handedness, and years of education. In our volumetric analyses, we additionally corrected for total cerebellar volume for cerebellar GM analyses and total intracranial volume (TIV) for cortical GM analyses. We evaluated the main effect of the Group (i.e., PLS/HC). To test for longitudinal differences in neuroimaging metric alterations over between PLS patients and HC, a linear mixed effects model was implemented using R's `nlme` package [32], where Time (i.e. session) was modelled as a random effect and the subjects as fixed effects. We corrected for the confounding effects of age, sex, handedness, and years of education. Volumetric analyses were also corrected for total cerebellar volumes (TCV) or total intracranial volumes (TIV) as appropriate, for cerebellar GM and cortical GM analyses respectively. We have evaluated the interaction effect "Time x Group" i.e., assessing if longitudinal progression was different in PLS compared to controls. Finally, we sought to compare whether disease burden was different in "cerebellar networks" compared to "primary motor networks". First, we extracted the coefficients for the main effect "Group"

(i.e., PLS vs. HC) from the ANOVA from all analysed ROIs and neuroimaging metrics (i.e., RD, FA, FC and volumetry), as described above. We then assigned, per neuroimaging metric, each ROI to the group “cerebellar network” or “primary motor network”. For example, for RD and FA, we compared the coefficients of the 11 assessed cerebellar tracts (i.e., bilateral cerebello-frontal/-parietal/-temporal/-occipital lobes/-thalamus and unified spinocerebellar) against the coefficients of three motor tracts (i.e., bilateral CST and transcallosal M1). To test for differential involvement of the two networks (supra- versus infratentorial), we used pairwise *t*-testing to test for means in the coefficients, regarding *p*-values < 0.05 as evidence of significant differences. Notice that for the volumetric analyses, *t*-testing was not possible since we only assessed volumetry for one ROI of the motor system (M1). Therefore, we provide instead descriptive statistics for the volumetric comparison. *T*-testing was performed within Matlab.

Data availability

Due to departmental policies, clinical, genetic or neuroimaging data from individual patients cannot be made available, but additional information can be requested from the corresponding author with regard to statistics and data processing pipelines.

Results

Subjects

In total, data from 43 PLS patients and 113 HC were assessed. For most subjects, longitudinal data with up to three follow-up sessions were available. Multimodal MRI data included T1w, dMRI and rs-fMRI data, whereby not for all subjects/sessions, all sequences were available. We provide further details on available/missing data in Table 1. Demographic data were compared between PLS patients and HC: Welch two-sample *t*-testing indicated appropriate matching for age ($t(80.33) = 1.33$, $p = 0.188$), however, PLS patients had significantly fewer years of education ($t(71.04) = -4.05$, $p = 0.001$). Chi-square tests revealed no differences in sex distributions between the groups ($X^2(1, N = 156) = 1.69$, $p = 0.193$), and in distributions of handedness ($X^2(1, N = 156) = 0.11$, $p = 0.736$). Patients with PLS tested negative for GGGGCC hexanucleotide expansions in *C9orf72* and the panel of HSP and ALS-associated genetic variants.

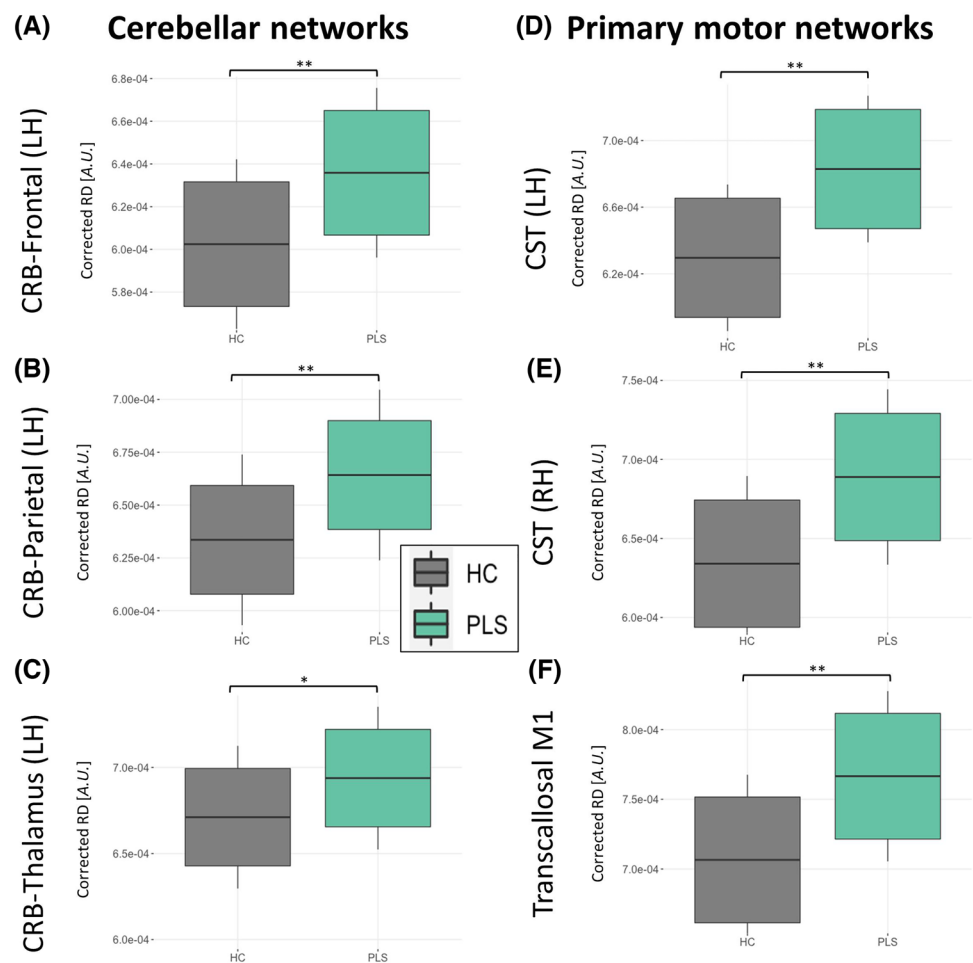
Cross-sectional findings at baseline

The PLS group exhibits infratentorial-supratentorial disconnection as compared to HC between the cerebellum and almost all lobes as well as the thalamus. This was found for both hemispheres and more evident for RD than FA. In Fig. 2, we present some illustrative RD findings between the cerebellum and frontal lobe (Fig. 2A), parietal lobe (Fig. 2B) and thalamus (Fig. 2C) tracts. With regards to the primary motor system, the CST (Fig. 2D–E) and trans-callosal tracts were also significantly affected (Fig. 2F) based on increased RD and decreased FA. Comprehensive descriptive statistics are provided in Table 2. and Fig. 3 highlights the key findings. The PLS groups display marked infratentorial/supratentorial disconnection, particularly between the cerebellum and parietal lobe (Fig. 3A) and the cerebellum and occipital lobes (Fig. 3B) in both hemispheres. Interestingly, the PLS group exhibits increased FC compared to HC between the cerebellum and LH frontal lobe (Fig. 3C). Unexpectedly, no FC differences were identified (Fig. 3D–F) in the primary motor system i.e. along the CST and CC. Further statistical details are provided in Table 2. Volume reductions were detected in PLS throughout the cerebellar cortex, including anterior (Fig. 4A) and posterior lobes, the vermis (Fig. 4B) and crura, but not in the flocculonodular lobe. We did not detect volumetric differences in the cerebellar nuclei, except for a tendency towards atrophy in the interposed nucleus (Fig. 4C). The motor cortex was significantly atrophic in PLS (Fig. 4D). Full statistics are provided in Table 2.

Longitudinal analyses

With regards to longitudinal structural connectivity, we found no evidence for divergent longitudinal progression between PLS and HC in any of the cerebellar (e.g., Fig. 5A for RD Cerebellum-to-parietal lobe, RH) or primary motor tracts (e.g., Fig. 5D for RD CST, RH). The results were similar for RD and FA. To assess differences in the evolution of FC, a linear mixed effects model was implemented to assess the interaction effect “Time x Group”, correcting for age, sex, handedness, and years of education. We found no evidence of accelerated FC disconnection in PLS compared to HC in any of the analyzed networks in cerebellar or primary motor circuits (Fig. 5E for FC of CST, RH). However, we detected a marked increase in FC in PLS over time between the cerebellum and RH parietal lobe (Fig. 5B). Differences in longitudinal volumetric trajectories between PLS and HC were also evaluated, but no significant differences were detected, neither for the cerebellar cortex (except for a tendency of accelerated atrophy of the flocculonodular lobe, Fig. 5C), cerebellar nuclei (not shown) or the motor cortex (e.g., Fig. 5F).

Fig. 2 Structural connectivity (SC) profiles at baseline in cerebellar (A–C) and primary motor networks (D–F) *indicates p -values $\leq .05$, **indicates p -values $\leq .001$, *CRB* Cerebellar



Divergent disease burden in the primary motor system and cerebellar networks

To test for disease burden differences between cerebellar and primary motor region, pairwise t-testing was used, comparing means of the coefficient of the main effect “Group” from all ROIs in each system. This analysis was repeated for each neuroimaging metric (Fig. 6). Baseline disease burden was more pronounced in the motor system as compared to the cerebellar system for SC, as evident by higher RD coefficients (Fig. 6A, $t(12) = -5.78$, $p < 0.001$) and lower FA coefficients (Fig. 6B, $t(12) = 5.16$, $p < 0.001$), but not for FC (Fig. 6C, $t(12) = -1.05$, $p = 0.312$). For the volumetric analysis (Fig. 6D), t-testing was not possible since only one value was available for the motor system. The mean/standard deviation of the volumetric coefficients of the assessed cerebellar ROIs was -0.258 ± 0.359 , the coefficient for M1 volumetry was -0.348 .

Discussion

Our data confirms considerable intra-cerebellar disease burden in PLS. We detected cerebello-frontal, temporal, parietal, occipital and cerebello-thalamic structural disconnection at baseline as well as impaired cerebello-frontal, -parietal and -occipital functional connectivity. Volume reductions were identified in the vermis, anterior lobe, posterior lobe, and crura. Among the deep cerebellar nuclei, the dorsal dentate was atrophic. Interestingly longitudinal follow-up did not capture statistically significant progressive changes. Consistent with classical imaging signatures, significant primary motor cortex atrophy and inter-hemispheric transcallosal degeneration was also captured based on diffusivity metrics but not based on functional analyses.

Table 2 Cross-sectional and longitudinal statistical comparisons of neuroimaging metrics between PLS and healthy controls

	Cross-sectional				Longitudinal (Interaction <i>Time x Group</i>)	
	Left hemisphere		Right hemisphere		Left hemisphere	Right hemisphere
	<i>F</i> -value (DOF)	<i>p</i> -value	<i>F</i> -value (DOF)	<i>p</i> -value	<i>t</i> -value (DOF), <i>p</i> -value	<i>t</i> -value (DOF), <i>p</i> -value
Connectivity: Crb-Frontal						
SC: RD	$F(1,146)=50.16$	<0.001**	$F(1,146)=56.89$	<0.001**	$t(110)=0.63$, $p=0.530$	$t(110)=1.30$, $p=0.197$
SC: FA	$F(1,146)=7.80$	0.006*	$F(1,146)=4.25$	0.041*	$t(110)=-0.92$, $p=0.358$	$t(110)=-1.93$, $p=.056$
FC	$F(1,142)=6.80$	0.010*	$F(1,142)=.782$	0.378	$t(101)=-1.16$, $p=0.249$	$t(101)=-0.01$, $p=0.991$
Connectivity: Crb-Parietal						
SC: RD	$F(1,146)=37.25$	<0.001**	$F(1,146)=36.28$	<0.001**	$t(110)=0.70$, $p=0.485$	$t(110)=-0.01$, $p=0.988$
SC: FA	$F(1,146)=2.22$	0.138	$F(1,146)=1.47$	0.228	$t(110)=-1.61$, $p=0.111$	$t(110)=-0.43$, $p=0.666$
FC	$F(1,142)=7.23$	0.008*	$F(1,142)=17.41$	<0.001**	$t(101)=1.50$, $p=0.138$	$t(101)=2.25$, $p=0.027^*$
Connectivity: Crb-Temporal						
SC: RD	$F(1,146)=10.44$	0.001**	$F(1,146)=25.68$	<0.001**	$t(110)=1.01$, $p=0.315$	$t(110)=0.05$, $p=0.958$
SC: FA	$F(1,146)=2.87$	0.092	$F(1,146)=3.09$	0.081	$t(109)=-0.66$, $p=0.508$	$t(109)=0.18$, $p=0.859$
FC	$F(1,142)=0.11$	0.738	$F(1,142)=0.20$	0.654	$t(101)=-1.75$, $p=0.084$	$t(101)=-0.72$, $p=0.473$
Connectivity: Crb-Occipital						
SC: RD	$F(1,146)=16.40$	<0.001**	$F(1,146)=31.84$	<0.001**	$t(110)=0.16$, $p=0.873$	$t(110)=-0.99$, $p=0.326$
SC: FA	$F(1,146)=0.30$	0.583	$F(1,146)=0.007$	0.933	$t(110)=0.17$, $p=0.864$	$t(110)=0.62$, $p=0.534$
FC	$F(1,142)=6.49$	0.012*	$F(1,142)=3.861$	0.051	$t(101)=-1.53$, $p=0.130$	$t(101)=0.29$, $p=0.772$
Connectivity: Crb-Thalamus						
SC: RD	$F(1,146)=5.21$	0.024*	$F(1,146)=3.44$	0.066	$t(110)=0.19$, $p=0.851$	$t(110)=0.44$, $p=0.658$
SC: FA	$F(1,146)=0.12$	0.728	$F(1,146)=0.07$	0.790	$t(110)=-0.06$, $p=0.955$	$t(110)=0.47$, $p=0.637$
FC	$F(1,142)=0.33$	0.566	$F(1,142)=2.45$	0.120	$t(101)=0.44$, $p=0.662$	$t(101)=0.84$, $p=0.404$
Connectivity: Spinocerebellar						
SC: RD	$F(1,146)=2.26$	0.135	n.a	n.a	$t(110)=-0.30$, $p=0.764$	n.a
SC: FA	$F(1,146)=1.18$	0.279	n.a	n.a	$t(110)=-0.65$, $p=0.515$	n.a
FC	$F(1,142)=0.33$	0.566	n.a	n.a	$t(101)=0.15$, $p=0.882$	n.a
Connectivity: Corticospinal tract						
SC: RD	$F(1,146)=50.30$	<0.001**	$F(1,146)=50.41$	<0.001**	$t(110)=1.06$, $p=0.289$	$t(110)=1.57$, $p=0.119$
SC: FA	$F(1,146)=27.64$	<0.001**	$F(1,146)=24.96$	<0.001**	$t(110)=1.06$, $p=0.289$	$t(110)=-1.74$, $p=0.084$
SC: FC	$F(1,142)=0.28$	0.596	$F(1,142)=0.32$	0.571	$t(101)=1.57$, $p=0.121$	$t(101)=0.04$, $p=0.970$
Connectivity: Transcallosal M1 (hemisphere n.a.)						

Table 2 (continued)

	Cross-sectional				Longitudinal (Interaction <i>Time x Group</i>)	
	Left hemisphere		Right hemisphere		Left hemisphere	Right hemisphere
	<i>F</i> -value (DOF)	<i>p</i> -value	<i>F</i> -value (DOF)	<i>p</i> -value	<i>t</i> -value (DOF), <i>p</i> -value	<i>t</i> -value (DOF), <i>p</i> -value
SC: RD	$F(1,146)=39.10$	<0.001**	n.a	n.a	$t(110)=1.85$, $p=0.066$	n.a
SC: FA	$F(1,146)=14.76$	0.002**	n.a	n.a	$t(110)=-1.05$, $p=0.297$	n.a
FC	$F(1,142)=0.63$	0.427	n.a	n.a	$t(101)=-0.96$, $p=0.340$	n.a
Volumetry: Cerebellar cortex (hemisphere: n.a.)						
Anterior cerebellar lobe	$F(1,146)=11.37$	<0.001**	n.a	n.a	$t(112)=-1.11$, $p=0.270$	n.a
Posterior cerebellar lobe	$F(1,146)=9.18$	0.002*	n.a	n.a	$t(112)=-1.27$, $p=0.208$	n.a
Flocculonodular lobe	$F(1,146)=1.04$	0.309	n.a	n.a	$t(112)=-1.85$, $p=0.067$	n.a
Cerebellar crura	$F(1,146)=5.02$	0.027*	n.a	n.a	$t(112)=-1.53$, $p=0.128$	n.a
Cerebellar vermis	$F(1,146)=5.51$	0.020*	n.a	n.a	$t(112)=-1.01$, $p=0.314$	n.a
Volumetry: Cerebellar nuclei (hemisphere: n.a.)						
Dorsal dentate nucleus	$F(1,146)=5.02$	0.027*	n.a	n.a	$t(112)=0.87$, $p=0.384$	n.a
Ventral dentate nucleus	$F(1,146)=1.21$	0.274	n.a	n.a	$t(112)=0.94$, $p=0.348$	n.a
Interposed nucleus	$F(1,146)=3.80$	0.053	n.a	n.a	$t(112)=0.78$, $p=.435$	n.a
Fastigial nucleus	$F(1,146)=0.41$	0.521	n.a	n.a	$t(112)=0.48$, $p=0.636$	n.a
Volumetry: Motor cortex (hemisphere: n.a.)						
M1	$F(1,146)=58.36$	<0.001**	n.a	n.a	$t(112)=-1.01$, $p=0.316$	n.a

ANOVA analysis of variance, *Crb* cerebellum, *dmMRI* diffusion-magnetic resonance imaging, *DOF* degrees of freedom, *FA* fractional anisotropy, *FC* functional connectivity, *HC* healthy control, *MI* primary motor cortex, *n.a.* not applicable, *RD* radial diffusivity, *PLS* primary lateral sclerosis, *rs-fMRI* resting-state functional MRI, *SC* structural connectivity, *T1w* T1-weighted MRI

*significant at an alpha-level of $p \leq 0.05$

**significant at an alpha-level of $p \leq 0.001$

Academic insights

Cortical cerebellar changes have been previously described in PLS, and our data also suggest widespread cerebellar grey matter change including the vermis, anterior lobe, posterior lobe, and crura. Posterior cerebellar pathology has been consistently linked to visuospatial, language, verbal memory, executive and sequencing deficits; while neuropsychological function may be relatively preserved with anterior cerebellar insults [68]. Cerebellar disease burden has also been linked to deficits in social cognition [69], language [70] and pseudobulbar affect [17, 20]. Vermis lesions may manifest emotional dysregulation such

as impulsivity, irritability, and disinhibition [71]. Previous imaging studies have reported cerebellar [9], spinocerebellar and dentato-rubro-thalamo-cortical (DRTC) tract diffusivity changes [72] as well as increased functional connectivity between the cerebellum and cortical motor, frontal and temporal areas [73]. Cognitive deficits in PLS have been linked to reduced FA and higher cerebellar RD [74]. Increased cerebro-cerebellar functional connectivity and expanded metabolic activation are also commonly reported in ALS [75, 76] and often interpreted as functional adaptation to neurodegenerative change [77, 78]. While concepts of neuroplasticity and compensatory mechanisms are attractive at a theoretical level, there is no compelling

Fig. 3 Functional connectivity (FC) profiles at baseline in cerebellar (A–C) and primary motor networks (D–E). *indicates p -values $\leq .05$, **indicates p -values $\leq .001$, *CRB* Cerebellar

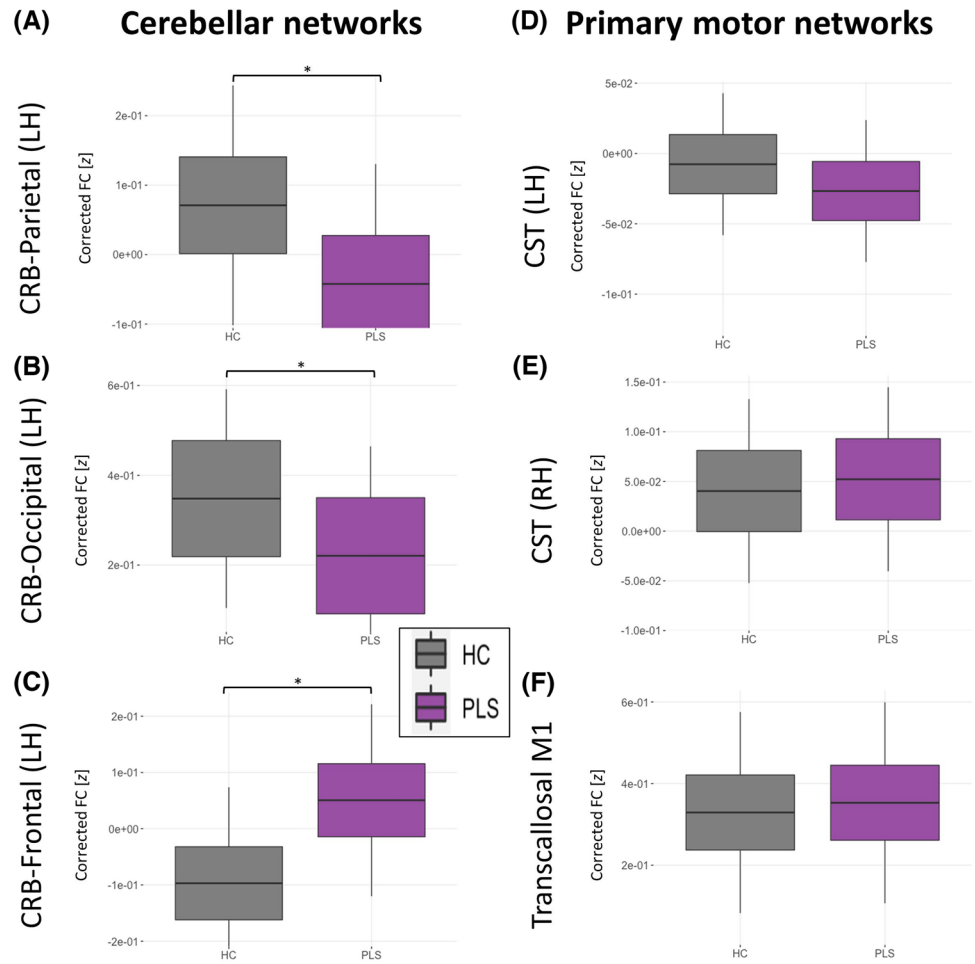


Fig. 4 Volumetric profiles at baseline in cerebellar structures (A–C) and in the primary motor cortex (D). *indicates p -values $\leq .05$, **indicates p -values $\leq .001$

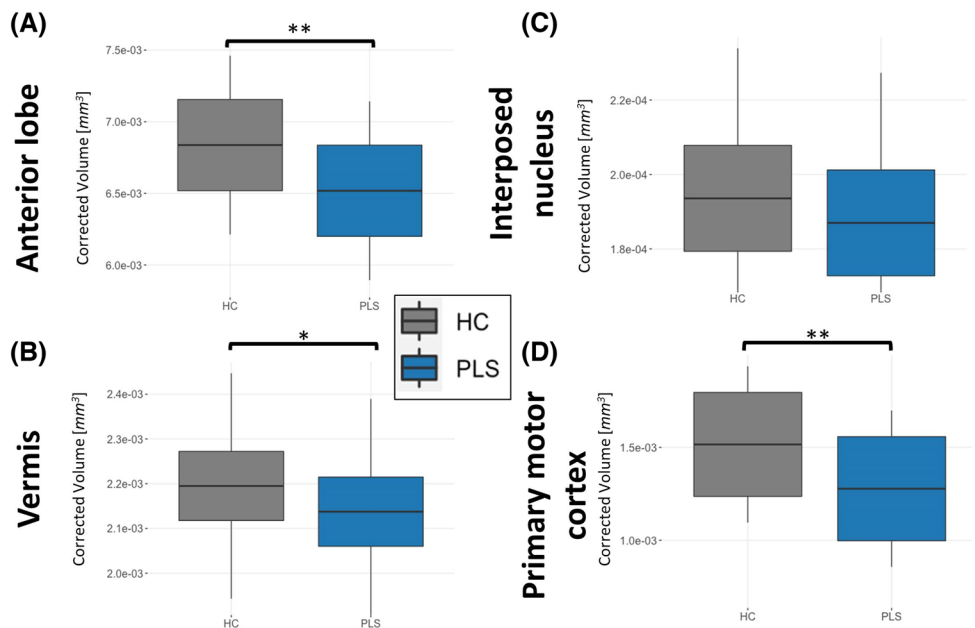
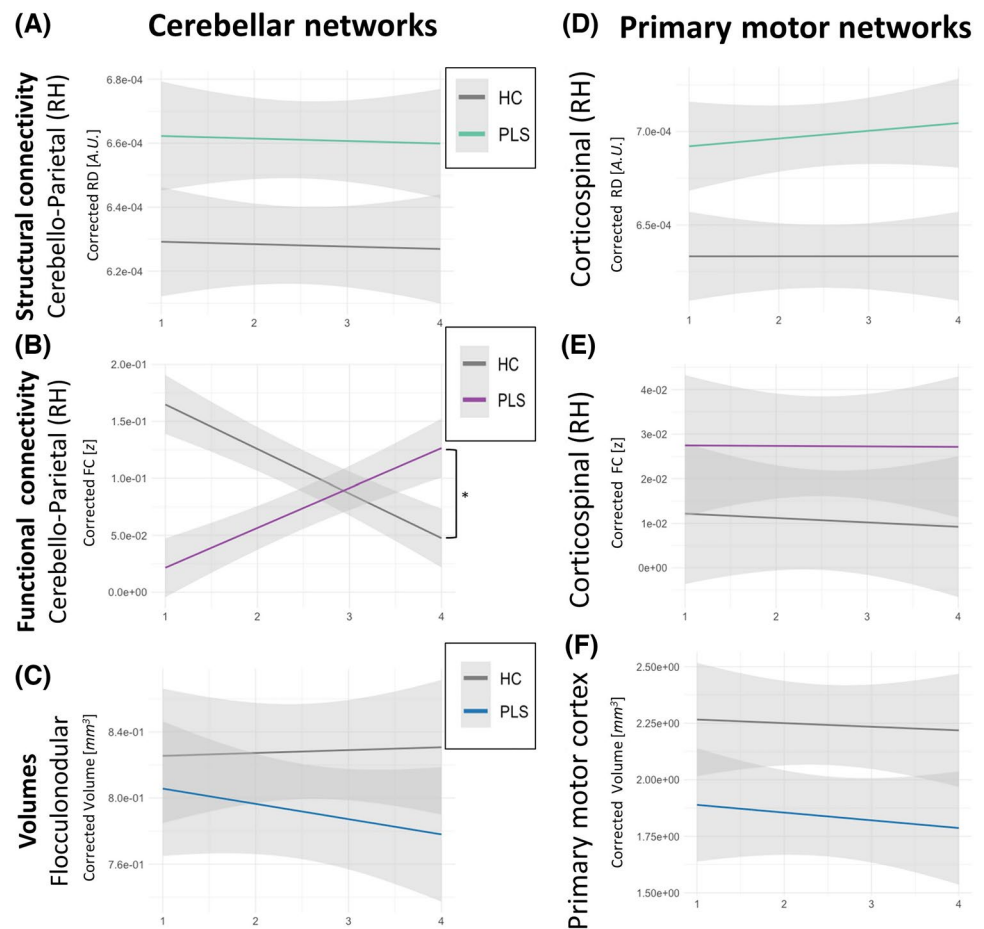


Fig. 5 The longitudinal evolution of cerebral and cerebellar integrity metrics. *indicates p -values $\leq .05$, **indicates p -values $\leq .001$



histopathology evidence to convincingly support adaptive structural processes [79].

Methodological considerations

From a methodological perspective, our results highlight the relative limitations of functional connectivity metrics. In our study, the detection sensitivity of structural connectivity indices clearly outperforms BOLD-signal-derived functional measures. This is potentially important for the design of short-duration clinical protocols, which should ideally only include pulse sequences with biomarker potential. While FA is the most widely evaluated diffusivity metric both in tractography and voxelwise models such as TBSS etc., our study highlights the importance of assessing other measures. In this study, RD was more sensitive to detect cortico-cerebellar disconnection than FA. It is noteworthy, that we did not detect significant longitudinal structural or functional changes, which is likely to stem from the long symptom duration profile of our sample. It is particularly striking that corticospinal tract, corpus callosum and primary motor cortex measures did not exhibit progressive decline either, despite the relentless clinical progression observed clinically.

This suggests a saturation-effect or ceiling effect of these variables i.e. while they capture significant differences with reference to control change there is no tangible further progression over time. One needs to also acknowledge the heterogeneity of the cohort with respect to symptom duration as well as the long average length of symptom duration. By the time these participants have been scanned they have had the disease for a long time, resulting in considerable CST, CC, and PMC degeneration which has not progressed further significantly during the relatively short 4-monthly follow-up periods. Accordingly, it would be particularly interesting to capture patients soon after symptom onset, before fulfilling diagnostic criteria or patients with “suspected” disease and evaluate their imaging change at a much earlier stage of the disease. We have made such attempts previously, evaluating patients with a symptom duration of 2–4 years i.e. patients with “probable PLS” according to the new consensus criteria [27] and they have already exhibited motor cortex and corticospinal tract alterations [28, 80]. Imaging patients with short symptom duration is particularly important as these are the patients who face diagnostic uncertainty, apprehensive about potentially developing ALS [81]. In this study, we used a single inferior (caudal) brainstem

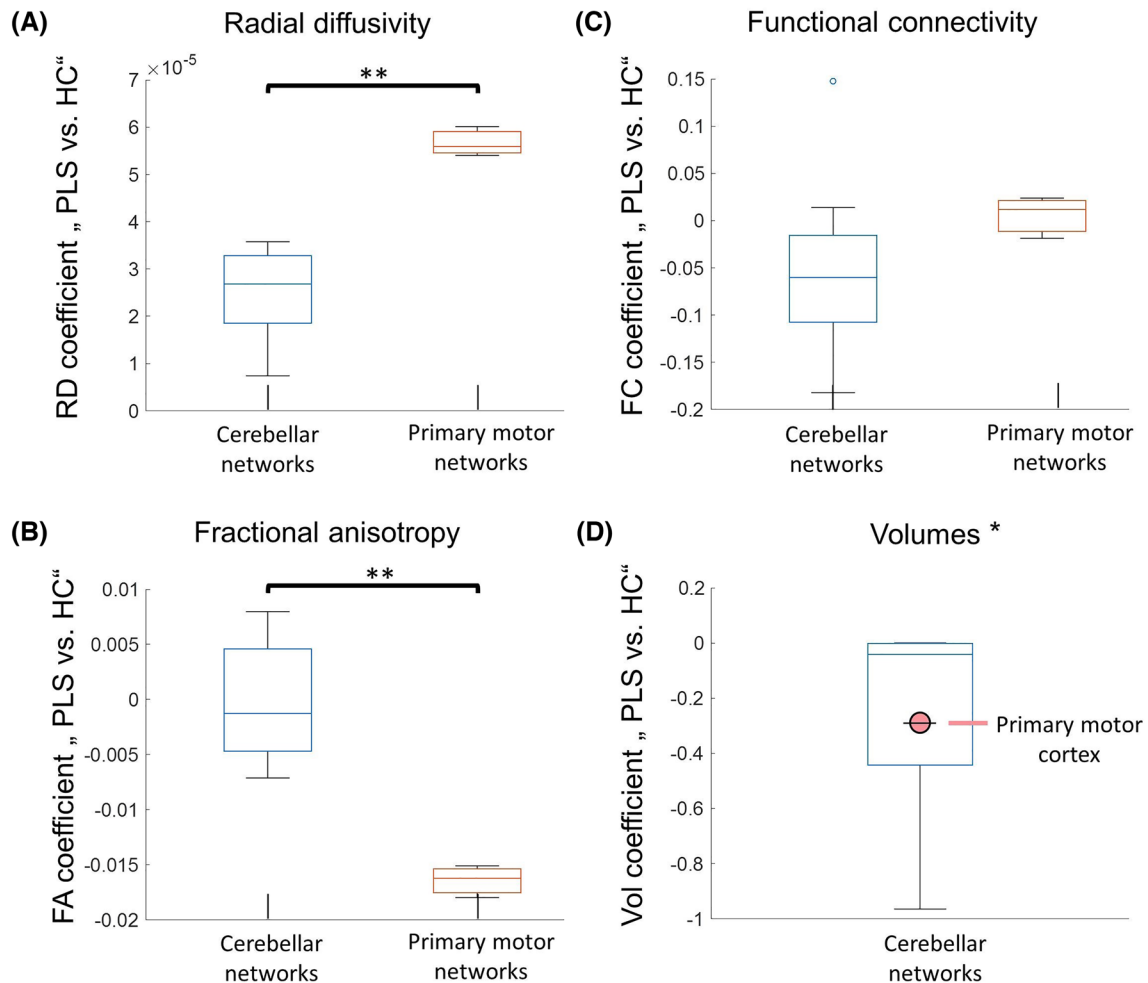


Fig. 6 The comparison of cerebral and cerebellar disease burden at baseline. *indicates p -values $\leq .05$, **indicates p -values $\leq .001$

mask to track ascending projections to the cerebellum as a proxy of the “spinocerebellar tracts”, but we concede that this is a suboptimal approach. High-resolution spinal data can now be reliably acquired with cardiac and respiratory gating in ALS [82] and correlated with clinical metrics [83, 84]. Spinal protocols in ALS have also been successfully utilised in diagnostic applications [85] and to describe presymptomatic changes in *C9orf72* [86]. Combined spinal and cerebral datasets are increasingly evaluated in ALS to accurately explore the substrate of clinical phenomena [83].

Clinical implications

From a pathophysiology standpoint, functional MRI studies in ALS [75, 77, 79] have consistently suggested that the cerebellum may assume a compensatory role in the face of supratentorial degeneration and cerebellar hypertrophy has also been detected in adult poliomyelitis survivors [87, 88]. In our study, PLS patients exhibit increased functional connectivity compared to controls between the cerebellum

and left frontal lobe at baseline (Fig. 3C) and increasing cerebello-parietal FC over time (Fig. 5B). As the increased FC is not supported by increased SC, one needs to be careful not to over-interpret BOLD synchronisation as proof of effective compensation. Our volumetric analyses revealed a trend for progressive flocculonodular lobe atrophy in PLS (Fig. 5). This region is a key hub of the vestibulo-ocular networks playing an important role in fixation, smooth pursuit, and vestibular responses to head motion. These observations support the importance of eye-movement assessments in PLS, particularly that other cerebellar manifestations, such as disequilibrium during stance and gait are affected by coexisting pyramidal weakness or spasticity. While eye-movement abnormalities have been extensively investigated in ALS [43], they are glaringly understudied in PLS. Cerebellar atrophy and cortico-cerebellar connectivity changes are also commonly observed in ALS, ALS-FTD and HSP [89–91]. Radiological measures are increasingly included as input features in machine-learning (ML) models in MNDs [92, 93], but these have only achieved

limited accuracy when distinguishing ALS from PLS on radiological grounds [94]. The development of accurate classification models that can successfully differentiate ALS from PLS soon after symptom onset is of utmost relevance given the strikingly different survival prospects in the two conditions [95]. From a clinical perspective, the specific contribution of cerebellar pathology to dexterity and gait impairment, dysarthria and dysphagia is difficult to demonstrate in the presence of considerable upper motor neuron dysfunction. Based on similar research studies in ALS, [76, 96], it is likely that extra-pyramidal [13] and cerebellar pathology in PLS [32] exacerbates motor disability in PLS. Accordingly, cerebellar components of motor disability should be considered in fall prevention, multidisciplinary rehabilitation, occupational, speech and physiotherapy.

Study limitations

This study is not without limitations. We acknowledge the relative heterogeneity of our sample with regards to symptom duration and that only 31 of the 43 patients had genomic data. We also concede that supplementary spectroscopy and PET data would have provided important complementary metabolic insights. Additional spinal MRI data would have permitted the direct evaluation of the spinocerebellar tracts instead of relying on an inferior brainstem mask for tractography. Notwithstanding these limitations, our data demonstrate considerable intra-cerebellar and well as significant cerebro-cerebellar connectivity alterations in PLS.

Conclusions

PLS is associated with considerable cerebellar disease burden; cortical atrophy, dorsal dentate degeneration and cerebro-cerebellar connectivity alterations. Cerebellar components of gait impairment, bulbar dysfunction and pseudobulbar affect in PLS should be carefully considered instead of attributing characteristic symptoms to primary motor cortex degeneration alone.

Supplementary Information The online version contains supplementary material available at <https://doi.org/10.1007/s00415-024-12261-z>.

Acknowledgements We are most thankful for the participation of each patient and healthy control, and we also thank all patients who expressed interest in this research study but were unable to participate for medical or logistical reasons. We also express our gratitude to the caregivers and families of individuals with PLS for facilitating attendance at our neuroimaging centre. Without their generosity this study would have not been possible.

Author contribution Conceptualisation of the study: MT, EET, EF, PB. Drafting the manuscript: JK, MT, EET, PB. Neuroimaging analyses: JK, MT, EET, SD, PB.

Clinical assessments: JK, SD, OH, EF, PB. Genetic analyses: JCH, MAD, RLMcL. Revision of the manuscript for intellectual content: JK, MT, EET, SD, JCH, MAD, RLMcL, OH, KMC, EF, PB.

Funding Open Access funding provided by the IReL Consortium. This study was sponsored by the Spastic Paraplegia Foundation, Inc. (SPF). Neuroimaging aspects of the project were also supported by the Health Research Board Ireland (JPND-Cofund-2-2019-1 & HRB EIA-2017-019), the EU Joint Programme – Neurodegenerative Disease Research (JPND), Science Foundation Ireland (SFI SP20/SP/8953), the Andrew Lydon scholarship, the Irish Institute of Clinical Neuroscience (IICN), and the Iris O’Brien Foundation. The genetic analyses of the study were supported by the MND Association (898–792) and Science Foundation Ireland (17/CDA/4737).

Declarations

Conflict of interest The authors of this manuscript have no conflicts of interest to disclose.

Ethical approval This study was approved by the Ethics (Medical Research) Committee—Beaumont Hospital, Dublin, Ireland.

Open Access This article is licensed under a Creative Commons Attribution 4.0 International License, which permits use, sharing, adaptation, distribution and reproduction in any medium or format, as long as you give appropriate credit to the original author(s) and the source, provide a link to the Creative Commons licence, and indicate if changes were made. The images or other third party material in this article are included in the article’s Creative Commons licence, unless indicated otherwise in a credit line to the material. If material is not included in the article’s Creative Commons licence and your intended use is not permitted by statutory regulation or exceeds the permitted use, you will need to obtain permission directly from the copyright holder. To view a copy of this licence, visit <http://creativecommons.org/licenses/by/4.0/>.

References

1. Carew JD, Nair G, Pineda-Alonso N, Usher S, Hu X, Benatar M (2011) Magnetic resonance spectroscopy of the cervical cord in amyotrophic lateral sclerosis. *Amyotrophic Lateral Scler* 12(3):185–191. <https://doi.org/10.3109/17482968.2010.515223>
2. Ta D, Ishaque AH, Elamy A, Anand T, Wu A, Eurich DT, Luk C, Yang YH, Kalra S (2023) Severity of in vivo corticospinal tract degeneration is associated with survival in amyotrophic lateral sclerosis: a longitudinal, multicohort study. *Eur J Neurol*. <https://doi.org/10.1111/ene.15686>
3. Ferraro PM, Agosta F, Riva N, Copetti M, Spinelli EG, Falzone Y, Sorarù G, Comi G, Chiò A, Filippi M (2017) Multimodal structural MRI in the diagnosis of motor neuron diseases. *NeuroImage Clinical* 16:240–247. <https://doi.org/10.1016/j.nicl.2017.08.002>
4. Pioro EP, Turner MR, Bede P (2020) Neuroimaging in primary lateral sclerosis. *Amyotrophic Lateral Scler Frontotemporal Degener* 21(sup1):18–27. <https://doi.org/10.1080/21678421.2020.1837176>
5. Clark MG, Smallwood Shoukry R, Huang CJ, Danielian LE, Bageac D, Floeter MK (2018) Loss of functional connectivity is an early imaging marker in primary lateral sclerosis. *Amyotrophic Lateral Scler Frontotemporal Degener*. <https://doi.org/10.1080/21678421.2018.1517180>

6. Floeter MK, Mills R (2009) Progression in primary lateral sclerosis: a prospective analysis. *Amyotroph Lateral Scler* 10(5–6):339–346
7. Tahedi M, Li Hi Shing S, Finegan E, Chipika RH, Lope J, Hardiman O, Bede P (2021) Propagation patterns in motor neuron diseases: individual and phenotype-associated disease-burden trajectories across the UMN-LMN spectrum of MNDs. *Neurobiol Aging* 109:78–87. <https://doi.org/10.1016/j.neurobiolaging.2021.04.031>
8. de Vries BS, Rustemeijer LMM, Bakker LA, Schröder CD, Veldink JH, van den Berg LH, Nijboer TCW, van Es MA (2019) Cognitive and behavioural changes in PLS and PMA: challenging the concept of restricted phenotypes. *J Neurol Neurosurg Psychiatry* 90(2):141–147. <https://doi.org/10.1136/jnnp-2018-318788>
9. Finegan E, Shing SLH, Chipika RH, Chang KM, McKenna MC, Doherty MA, Hengeveld JC, Vajda A, Pender N, Donaghy C, Hutchinson S, McLaughlin RL, Hardiman O, Bede P (2021) Extra-motor cerebral changes and manifestations in primary lateral sclerosis. *Brain Imaging Behav*. <https://doi.org/10.1007/s11682-020-00421-4>
10. Le Forestier N, Maisonobe T, Piquard A, Rivaud S, Crevier-Buchman L, Salachas F, Pradat PF, Lacomblez L, Meininger V (2001) Does primary lateral sclerosis exist? A study of 20 patients and a review of the literature. *Brain: J Neurol* 124(Pt 10):1989–1999
11. Bede P, Pradat PF, Lope J, Vourc'h P, Blasco H, Corcia P (2021) Primary lateral sclerosis: clinical, radiological and molecular features. *Rev Neurol*. <https://doi.org/10.1016/j.neurol.2021.04.008>
12. de Vries BS, Spreij LA, Rustemeijer LMM, Bakker LA, Veldink JH, van den Berg LH, Nijboer TCW, van Es MA (2019) A neuropsychological and behavioral study of PLS. *Amyotrophic Lateral Scler Frontotemporal Degener* 20(5–6):376–384. <https://doi.org/10.1080/21678421.2019.1620284>
13. Finegan E, Li Hi Shing S, Chipika RH, Doherty MA, Hengeveld JC, Vajda A, Donaghy C, Pender N, McLaughlin RL, Hardiman O, Bede P (2019) Widespread subcortical grey matter degeneration in primary lateral sclerosis: a multimodal imaging study with genetic profiling. *NeuroImage Clin* 24:102089. <https://doi.org/10.1016/j.nicl.2019.102089>
14. Chipika RH, Christidi F, Finegan E, Li Hi Shing S, McKenna MC, Chang KM, Karavasilis E, Doherty MA, Hengeveld JC, Vajda A, Pender N, Hutchinson S, Donaghy C, McLaughlin RL, Hardiman O, Bede P (2020) Amygdala pathology in amyotrophic lateral sclerosis and primary lateral sclerosis. *J Neurol Sci* 417:117039. <https://doi.org/10.1016/j.jns.2020.117039>
15. Chipika RH, Finegan E, Li Hi Shing S, McKenna MC, Christidi F, Chang KM, Doherty MA, Hengeveld JC, Vajda A, Pender N, Hutchinson S, Donaghy C, McLaughlin RL, Hardiman O, Bede P (2020) “Switchboard” malfunction in motor neuron diseases: selective pathology of thalamic nuclei in amyotrophic lateral sclerosis and primary lateral sclerosis. *NeuroImage Clin* 27:102300. <https://doi.org/10.1016/j.nicl.2020.102300>
16. Hubers A, Kassubek J, Gron G, Gorges M, Aho-Oezhan H, Keller J, Horn H, Neugebauer H, Uttner I, Lule D, Ludolph AC (2016) Pathological laughing and crying in amyotrophic lateral sclerosis is related to frontal cortex function. *J Neurol* 263(9):1788–1795. <https://doi.org/10.1007/s00415-016-8201-5>
17. Bede P, Finegan E (2018) Revisiting the pathoanatomy of pseudobulbar affect: mechanisms beyond corticobulbar dysfunction. *Amyotrophic Lateral Scler Frontotemporal Degener* 19(1–2):4–6. <https://doi.org/10.1080/21678421.2017.1392578>
18. Parvizi J, Anderson SW, Martin CO, Damasio H, Damasio AR (2001) Pathological laughter and crying: a link to the cerebellum. *Brain: J Neurol* 124(Pt 9):1708–1719
19. Floeter MK, Katipally R, Kim MP, Schanz O, Stephen M, Danielian L, Wu T, Huey ED, Meoded A (2014) Impaired corticopontocerebellar tracts underlie pseudobulbar affect in motor neuron disorders. *Neurology* 83(7):620–627. <https://doi.org/10.1212/wnl.0000000000000693>
20. Finegan E, Chipika RH, Li Hi Shing S, Hardiman O, Bede P (2019) Pathological crying and laughing in motor neuron disease: pathobiology, screening. *Intervention Front Neurol* 10:260. <https://doi.org/10.3389/fneur.2019.00260>
21. Argyropoulos GD, Christidi F, Karavasilis E, Velonakis G, Antoniou A, Bede P, Seimenis I, Kelekis N, Douzenis A, Papakonstantinou O, Efstathopoulos E, Ferentinos P (2021) Cerebro-cerebellar white matter connectivity in bipolar disorder and associated polarity subphenotypes. *Prog Neuropsychopharmacol Biol Psychiatry* 104:110034. <https://doi.org/10.1016/j.pnpbp.2020.110034>
22. Christidi F, Karavasilis E, Ferentinos P, Xirou S, Velonakis G, Rentzos M, Zouvelou V, Zalonis I, Efstathopoulos E, Kelekis N, Evdokimidis I (2017) Investigating the neuroanatomical substrate of pathological laughing and crying in amyotrophic lateral sclerosis with multimodal neuroimaging techniques. *Amyotrophic Lateral Scler Frontotemporal Degener*. <https://doi.org/10.1080/21678421.2017.1386689>
23. Trojsi F, Di Nardo F, D'Alvano G, Caiazzo G, Passaniti C, Mangione A, Sharbafshaaer M, Russo A, Silvestro M, Siciliano M, Cirillo M, Tedeschi G, Esposito F (2023) Resting state fMRI analysis of pseudobulbar affect in amyotrophic lateral sclerosis (ALS): motor dysfunction of emotional expression. *Brain Imaging Behav* 17(1):77–89. <https://doi.org/10.1007/s11682-022-00744-4>
24. Finegan E, Chipika RH, Doherty MA, McLaughlin RL, Iyer PM, Donaghy C, Hardiman O, Bede P (2018) Primary lateral sclerosis, part of the MND spectrum or distinct entity: a multiparametric neuroimaging study with comprehensive clinical and genetic profiling. *Amyotrophic Lateral Scler Frontotemporal Degener* 19:11–12. <https://doi.org/10.1080/21678421.2018.1510202>
25. Tahedi M, Tan EL, Shing SLH, Chipika RH, Siah WF, Hengeveld JC, Doherty MA, McLaughlin RL, Hardiman O, Finegan E, Bede P (2023) Not a benign motor neuron disease: longitudinal imaging captures relentless motor connectome disintegration in primary lateral sclerosis. *Eur J Neurol* 30(5):1232–1245. <https://doi.org/10.1111/ene.15725>
26. Mackenzie IRA, Briemberg H (2020) TDP-43 pathology in primary lateral sclerosis. *Amyotrophic Lateral Scler Frontotemporal Degener* 21(sup1):52–58. <https://doi.org/10.1080/21678421.2020.1790607>
27. Turner MR, Barohn RJ, Corcia P, Fink JK, Harms MB, Kiernan MC, Ravits J, Silani V, Simmons Z, Statland J, van den Berg LH, Mitsumoto H (2020) Primary lateral sclerosis: consensus diagnostic criteria. *J Neurol Neurosurg Psychiatry* 91(4):373–377. <https://doi.org/10.1136/jnnp-2019-322541>
28. Finegan E, Siah WF, Shing SLH, Chipika RH, Chang KM, McKenna MC, Doherty MA, Hengeveld JC, Vajda A, Donaghy C, Hutchinson S, McLaughlin RL, Hardiman O, Bede P (2020) Imaging and clinical data indicate considerable disease burden in ‘probable’ PLS: patients with UMN symptoms for 2–4 years. *Data Brief*. <https://doi.org/10.1016/j.dib.2020.106247>
29. Tan CF, Kakita A, Piao YS, Kikugawa K, Endo K, Tanaka M, Okamoto K, Takahashi H (2003) Primary lateral sclerosis: a rare upper-motor-predominant form of amyotrophic lateral sclerosis often accompanied by frontotemporal lobar degeneration with ubiquitinated neuronal inclusions? Report of an autopsy case and a review of the literature. *Acta Neuropathol* 105(6):615–620
30. Canu E, Agosta F, Galantucci S, Chio A, Riva N, Silani V, Falini A, Comi G, Filippi M (2013) Extramotor damage is associated with cognition in primary lateral sclerosis patients. *PLoS ONE [Electronic Resource]* 8(12):e82017
31. Finegan E, Chipika RH, Li Hi Shing S, Doherty MA, Hengeveld JC, Vajda A, Donaghy C, McLaughlin RL, Pender N, Hardiman O, Bede P (2019) The clinical and radiological profile of

- primary lateral sclerosis: a population-based study. *J Neurol* 266(11):2718–2733. <https://doi.org/10.1007/s00415-019-09473-z>
32. Finegan E, Siah WF, Li Hi Shing S, Chipika RH, Hardiman O, Bede P (2022) Cerebellar degeneration in primary lateral sclerosis: an under-recognized facet of PLS. *Amyotrophic Lateral Scler Frontotemporal Degener*. <https://doi.org/10.1080/21678421.2021.2023188>
 33. Agosta F, Galantucci S, Riva N, Chio A, Messina S, Iannaccone S, Calvo A, Silani V, Copetti M, Falini A, Comi G, Filippi M (2014) Intrahemispheric and interhemispheric structural network abnormalities in PLS and ALS. *Hum Brain Mapp* 35(4):1710–1722
 34. Meoded A, Morrisette AE, Katipally R, Schanz O, Gotts SJ, Floeter MK (2015) Cerebro-cerebellar connectivity is increased in primary lateral sclerosis. *NeuroImage Clinical* 7:288–296
 35. Tu S, Menke RAL, Talbot K, Kiernan MC, Turner MR (2019) Cerebellar tract alterations in PLS and ALS. *Amyotrophic Lateral Scler Frontotemporal Degener* 20(3–4):281–284. <https://doi.org/10.1080/21678421.2018.1562554>
 36. Bede P, Chipika RH, Finegan E, Li Hi Shing S, Doherty MA, Hengeveld JC, Vajda A, Hutchinson S, Donaghy C, McLaughlin RL, Hardiman O (2019) Brainstem pathology in amyotrophic lateral sclerosis and primary lateral sclerosis: a longitudinal neuroimaging study. *NeuroImage Clin* 24:102054. <https://doi.org/10.1016/j.nicl.2019.102054>
 37. Bede P, Chipika RH, Finegan E, Li Hi Shing S, Chang KM, Doherty MA, Hengeveld JC, Vajda A, Hutchinson S, Donaghy C, McLaughlin RL, Hardiman O (2020) Progressive brainstem pathology in motor neuron diseases: imaging data from amyotrophic lateral sclerosis and primary lateral sclerosis. *Data Brief* 29:105229. <https://doi.org/10.1016/j.dib.2020.105229>
 38. Barohn RJ, Fink JK, Heiman-Patterson T, Huey ED, Murphy J, Statland JM, Turner MR, Elman L (2020) The clinical spectrum of primary lateral sclerosis. *Amyotrophic Lateral Scler Frontotemporal Degener* 21(sup1):3–10. <https://doi.org/10.1080/21678421.2020.1837178>
 39. Chipika RH, Mulkerrin G, Pradat PF, Murad A, Ango F, Raoul C, Bede P (2022) Cerebellar pathology in motor neuron disease: neuroplasticity and neurodegeneration. *Neural Regen Res* 17(11):2335–2341. <https://doi.org/10.4103/1673-5374.336139>
 40. Bede P, Chipika RH, Christidi F, Hengeveld JC, Karavasilis E, Argyropoulos GD, Lope J, Li Hi Shing S, Velonakis G, Dupuis L, Doherty MA, Vajda A, McLaughlin RL, Hardiman O (2021) Genotype-associated cerebellar profiles in ALS: focal cerebellar pathology and cerebro-cerebellar connectivity alterations. *J Neurol Neurosurg Psychiatry* 92(11):1197–1205. <https://doi.org/10.1136/jnnp-2021-326854>
 41. Floeter MK, Warden D, Lange D, Wymer J, Paganoni S, Mitsumoto H (2020) Clinical care and therapeutic trials in PLS. *Amyotrophic Lateral Scler Frontotemporal Degener* 21(sup1):67–73. <https://doi.org/10.1080/21678421.2020.1837180>
 42. Donaghy C, Thurtell MJ, Pioro EP, Gibson JM, Leigh RJ (2011) Eye movements in amyotrophic lateral sclerosis and its mimics: a review with illustrative cases. *J Neurol Neurosurg Psychiatry* 82(1):110–116. <https://doi.org/10.1136/jnnp.2010.212407>
 43. Proudfoot M, Menke RAL, Sharma R, Berna CM, Hicks SL, Kennard C, Talbot K, Turner MR (2015) Eye-tracking in amyotrophic lateral sclerosis: a longitudinal study of saccadic and cognitive tasks. *Amyotrophic Lateral Scler Frontotemporal Degener* 17(1–2):101–111. <https://doi.org/10.3109/21678421.2015.1054292>
 44. Malm J, Kristensen B, Karlsson T, Carlberg B, Fagerlund M, Olsson T (1998) Cognitive impairment in young adults with infratentorial infarcts. *Neurology* 51(2):433–440. <https://doi.org/10.1212/wnl.51.2.433>
 45. Yunusova Y, Plowman EK, Green JR, Barnett C, Bede P (2019) Clinical measures of bulbar dysfunction in ALS. *Front Neurol* 10:106. <https://doi.org/10.3389/fneur.2019.00106>
 46. Sasegbon A, Hamdy S (2021) The role of the cerebellum in swallowing. *Dysphagia*. <https://doi.org/10.1007/s00455-021-10271-x>
 47. Stoodley CJ, Schmahmann JD (2009) Functional topography in the human cerebellum: a meta-analysis of neuroimaging studies. *Neuroimage* 44(2):489–501. <https://doi.org/10.1016/j.neuroimage.2008.08.039>
 48. Argyropoulos GPD, van Dun K, Adamaszek M, Leggio M, Manto M, Masciullo M, Molinari M, Stoodley CJ, Van Overwalle F, Ivry RB, Schmahmann JD (2020) The cerebellar cognitive affective/schmahmann syndrome: a task force paper. *Cerebellum* 19(1):102–125. <https://doi.org/10.1007/s12311-019-01068-8>
 49. Christidi F, Karavasilis E, Rentzos M, Kelekis N, Evdokimidis I, Bede P (2018) Clinical and radiological markers of extra-motor deficits in amyotrophic lateral sclerosis. *Front Neurol* 9:1005. <https://doi.org/10.3389/fneur.2018.01005>
 50. Burke T, Pinto-Grau M, Lonergan K, Elamin M, Bede P, Costello E, Hardiman O, Pender N (2016) Measurement of social cognition in amyotrophic lateral sclerosis: a population based study. *PLoS ONE* 11(8):e0160850. <https://doi.org/10.1371/journal.pone.0160850>
 51. Burke T, Elamin M, Bede P, Pinto-Grau M, Lonergan K, Hardiman O, Pender N (2016) Discordant performance on the “Reading the Mind in the Eyes” Test, based on disease onset in amyotrophic lateral sclerosis. *Amyotrophic Lateral Scler Frontotemporal Degener*. <https://doi.org/10.1080/21678421.2016.1177088>
 52. Finegan E, Shing SLH, Chipika RH, Chang KM, McKenna MC, Doherty MA, Hengeveld JC, Vajda A, Pender N, Donaghy C, Hutchinson S, McLaughlin RL, Hardiman O, Bede P (2021) Extra-motor cerebral changes and manifestations in primary lateral sclerosis. *Brain Imaging Behav* 15(5):2283–2296. <https://doi.org/10.1007/s11682-020-00421-4>
 53. Abel O, Shatunov A, Jones AR, Andersen PM, Powell JF, Al-Chalabi A (2013) Development of a smartphone app for a genetics website: the amyotrophic lateral sclerosis online genetics database (ALSoD). *JMIR Mhealth Uhealth* 1(2):e18–e18. <https://doi.org/10.2196/mhealth.2706>
 54. Klebe S, Stevanin G, Depienne C (2015) Clinical and genetic heterogeneity in hereditary spastic paraplegias: from SPG1 to SPG72 and still counting. *Rev Neurol* 171(6–7):505–530. <https://doi.org/10.1016/j.neurol.2015.02.017>
 55. Gaser C, Dahnke R, Thompson PM, Kurth F, Luders E, Initiative AsDN (2023) CAT – a computational anatomy toolbox for the analysis of structural MRI data. *Biorxiv*. <https://doi.org/10.1101/2022.06.11.495736>
 56. Diedrichsen J (2006) A spatially unbiased atlas template of the human cerebellum. *Neuroimage* 33(1):127–138. <https://doi.org/10.1016/j.neuroimage.2006.05.056>
 57. Amunts K, Mohlberg H, Bludau S, Zilles K (2020) Julich-brain: a 3D probabilistic atlas of the human brain’s cytoarchitecture. *Science* 369(6506):988–992. <https://doi.org/10.1126/science.abb4588>
 58. Eickhoff SB, Stephan KE, Mohlberg H, Grefkes C, Fink GR, Amunts K, Zilles K (2005) A new SPM toolbox for combining probabilistic cytoarchitectonic maps and functional imaging data. *Neuroimage* 25(4):1325–1335. <https://doi.org/10.1016/j.neuroimage.2004.12.034>
 59. Tournier J-D, Calamante F, Connelly A (2012) MRtrix: diffusion tractography in crossing fiber regions. *Int J Imaging Syst Technol* 22(1):53–66. <https://doi.org/10.1002/ima.22005>
 60. Tournier JD, Calamante F, Connelly A (2007) Robust determination of the fibre orientation distribution in diffusion MRI: non-negativity constrained super-resolved spherical deconvolution.

- Neuroimage 35(4):1459–1472. <https://doi.org/10.1016/j.neuroimage.2007.02.016>
61. Raffelt D, Dhollander T, Tournier JD, Tabbara R, Smith R, Pierre E, Connelly A (2017) Bias field correction and intensity normalisation for quantitative analysis of apparent fibre density. *Proc ISMRM* 26:3541
 62. Tzourio-Mazoyer N, Landeau B, Papathanassiou D, Crivello F, Etard O, Delcroix N, Mazoyer B, Joliot M (2002) Automated anatomical labelling of activations in SPM using a macroscopic anatomical parcellation of the MNI MRI single-subject brain. *Neuroimage* 15(1):273–289. <https://doi.org/10.1006/nimg.2001.0978>
 63. Tournier JD, Calamante F, Connelly A (2010) Improved probabilistic streamlines tractography by 2nd order integration over fibre orientation distributions. *Proceedings of the international society for magnetic resonance in medicine (ISMRM)* 18
 64. Calamante F, Tournier JD, Jackson GD, Connelly A (2010) Track-density imaging (TDI): super-resolution white matter imaging using whole-brain track-density mapping. *Neuroimage* 53(4):1233–1243. <https://doi.org/10.1016/j.neuroimage.2010.07.024>
 65. Jenkinson M, Beckmann CF, Behrens TEJ, Woolrich MW, Smith SM (2012) FSL. *Neuroimage* 62(2):782–790. <https://doi.org/10.1016/j.neuroimage.2011.09.015>
 66. Pruim RHR, Mennes M, van Rooij D, Llera A, Buitelaar JK, Beckmann CF (2015) ICA-AROMA: a robust ICA-based strategy for removing motion artifacts from fMRI data. *Neuroimage* 112:267–277. <https://doi.org/10.1016/j.neuroimage.2015.02.064>
 67. Oosterhof NN, Connolly AC, Haxby JV (2016) CoSMoMVPA: multi-modal multivariate pattern analysis of neuroimaging data in matlab/GNU octave. *Front Neuroinform* 10:27. <https://doi.org/10.3389/fninf.2016.00027>
 68. Tedesco AM, Chiricozzi FR, Clausi S, Lupo M, Molinari M, Leggio MG (2011) The cerebellar cognitive profile. *Brain* 134(12):3672–3686. <https://doi.org/10.1093/brain/awr266>
 69. Van Overwalle F, D'Aes T, Marien P (2015) Social cognition and the cerebellum: a meta-analytic connectivity analysis. *Hum Brain Mapp* 36(12):5137–5154. <https://doi.org/10.1002/hbm.23002>
 70. Runnqvist E, Bonnard M, Gauvin HS, Attarian S, Trébuchon A, Hartsuiker RJ, Alario FX (2016) Internal modeling of upcoming speech: a causal role of the right posterior cerebellum in non-motor aspects of language production. *Cortex* 81:203–214. <https://doi.org/10.1016/j.cortex.2016.05.008>
 71. Levisohn L, Cronin-Golomb A, Schmahmann JD (2000) Neuropsychological consequences of cerebellar tumour resection in children: cerebellar cognitive affective syndrome in a paediatric population. *Brain* 123(5):1041–1050. <https://doi.org/10.1093/brain/123.5.1041>
 72. Tu S, Menke RAL, Talbot K, Kiernan MC, Turner MR (2019) Cerebellar tract alterations in PLS and ALS. *Amyotroph Lateral Scler Frontotemporal Degener* 20(3–4):281–284. <https://doi.org/10.1080/21678421.2018.1562554>
 73. Meoded A, Morrisette AE, Katipally R, Schanz O, Gotts SJ, Floeter MK (2015) Cerebro-cerebellar connectivity is increased in primary lateral sclerosis. *Neuroimage Clin* 7:288–296. <https://doi.org/10.1016/j.nicl.2014.12.009>
 74. Canu E, Agosta F, Galantucci S, Chiò A, Riva N, Silani V, Falini A, Comi G, Filippi M (2013) Extramotor damage is associated with cognition in primary lateral sclerosis patients. *PLoS ONE* 8(12):e82017. <https://doi.org/10.1371/journal.pone.0082017>
 75. Proudfoot M, Bede P, Turner MR (2018) Imaging cerebral activity in amyotrophic lateral sclerosis. *Front Neurol* 9:1148. <https://doi.org/10.3389/fneur.2018.01148>
 76. Abidi M, de Marco G, Grami F, Termoz N, Couillandre A, Querin G, Bede P, Pradat PF (2021) Neural correlates of motor imagery of gait in amyotrophic lateral sclerosis. *J Magn Reson Imaging* 53(1):223–233. <https://doi.org/10.1002/jmri.27335>
 77. Abidi M, de Marco G, Couillandre A, Feron M, Mseddi E, Termoz N, Querin G, Pradat PF, Bede P (2020) Adaptive functional reorganization in amyotrophic lateral sclerosis: coexisting degenerative and compensatory changes. *Eur J Neurol* 27(1):121–128. <https://doi.org/10.1111/ene.14042>
 78. Prell T, Grosskreutz J (2013) The involvement of the cerebellum in amyotrophic lateral sclerosis. *Amyotroph Lateral Scler Frontotemporal Degener* 14(7–8):507–515. <https://doi.org/10.3109/21678421.2013.812661>
 79. Bede P, Bogdahn U, Lope J, Chang KM, Xirou S, Christidi F (2021) Degenerative and regenerative processes in amyotrophic lateral sclerosis: motor reserve, adaptation and putative compensatory changes. *Neural Regen Res* 16(6):1208–1209. <https://doi.org/10.4103/1673-5374.300440>
 80. Finegan E, Li Hi Shing S, Siah WF, Chipika RH, Chang KM, McKenna MC, Doherty MA, Hengeveld JC, Vajda A, Donaghy C, Hutchinson S, McLaughlin RL, Hardiman O, Bede P (2020) Evolving diagnostic criteria in primary lateral sclerosis: the clinical and radiological basis of “probable PLS.” *J Neurol Sci* 417:117052. <https://doi.org/10.1016/j.jns.2020.117052>
 81. Finegan E, Chipika RH, Shing SLH, Hardiman O, Bede P (2019) Primary lateral sclerosis: a distinct entity or part of the ALS spectrum? *Amyotroph Lateral Scler Frontotemporal Degener* 20(3–4):133–145. <https://doi.org/10.1080/21678421.2018.1550518>
 82. El Mendili MM, Querin G, Bede P, Pradat PF (2019) Spinal cord imaging in amyotrophic lateral sclerosis: historical concepts-novel techniques. *Front Neurol* 10:350. <https://doi.org/10.3389/fneur.2019.00350>
 83. Khamaysa M, Lefort M, Pélégriani-Issac M, Lackmy-Vallée A, Mendili MME, Preuilh A, Devos D, Bruneteau G, Salachas F, Lenglet T, Amador MM, Le Forestier N, Hesters A, Gonzalez J, Rolland AS, Desnuelle C, Chupin M, Querin G, Georges M, Morelot-Panzini C, Marchand-Pauvert V, Pradat PF (2023) Quantitative brainstem and spinal MRI in amyotrophic lateral sclerosis: implications for predicting noninvasive ventilation needs. *J Neurol*. <https://doi.org/10.1007/s00415-023-12045-x>
 84. Bede P, Bokde AL, Byrne S, Elamin M, Fagan AJ, Hardiman O (2012) Spinal cord markers in ALS: diagnostic and biomarker considerations. *Amyotroph Lateral Scler* 13(5):407–415. <https://doi.org/10.3109/17482968.2011.649760>
 85. Querin G, El Mendili MM, Bede P, Delphine S, Lenglet T, Marchand-Pauvert V, Pradat PF (2018) Multimodal spinal cord MRI offers accurate diagnostic classification in ALS. *J Neurol Neurosurg Psychiatry* 89(11):1220–1221. <https://doi.org/10.1136/jnnp-2017-317214>
 86. Querin G, Bede P, El Mendili MM, Li M, Pelegrini-Issac M, Rinaldi D, Catala M, Saracino D, Salachas F, Camuzat A, Marchand-Pauvert V, Cohen-Adad J, Colliot O, Le Ber I, Pradat PF (2019) Presymptomatic spinal cord pathology in c9orf72 mutation carriers: a longitudinal neuroimaging study. *Ann Neurol* 86(2):158–167. <https://doi.org/10.1002/ana.25520>
 87. Li Hi Shing S, Lope J, McKenna MC, Chipika RH, Hardiman O, Bede P (2021) Increased cerebral integrity metrics in poliomyelitis survivors: putative adaptation to longstanding lower motor neuron degeneration. *J Neurol Sci* 424:117361. <https://doi.org/10.1016/j.jns.2021.117361>
 88. Li Hi Shing S, Lope J, Chipika RH, Hardiman O, Bede P (2021) Imaging data indicate cerebral reorganisation in poliomyelitis survivors: Possible compensation for longstanding lower motor neuron pathology. *Data Brief* 38:107316. <https://doi.org/10.1016/j.dib.2021.107316>
 89. McKenna MC, Chipika RH, Li Hi Shing S, Christidi F, Lope J, Doherty MA, Hengeveld JC, Vajda A, McLaughlin RL, Hardiman O, Hutchinson S, Bede P (2021) Infratentorial pathology in

- frontotemporal dementia: cerebellar grey and white matter alterations in FTD phenotypes. *J Neurol* 268(12):4687–4697. <https://doi.org/10.1007/s00415-021-10575-w>
90. McKenna MC, Tahedl M, Murad A, Lope J, Hardiman O, Hutchinson S, Bede P (2022) White matter microstructure alterations in frontotemporal dementia: phenotype-associated signatures and single-subject interpretation. *Brain Behav* 12(2):e2500. <https://doi.org/10.1002/brb3.2500>
91. Mulkerrin G, França MC Jr, Lope J, Tan EL, Bede P (2022) Neuroimaging in hereditary spastic paraplegias: from qualitative cues to precision biomarkers. *Expert Rev Mol Diagn* 22(7):745–760. <https://doi.org/10.1080/14737159.2022.2118048>
92. Bede P, Chang KM, Tan EL (2022) Machine-learning in motor neuron diseases: prospects and pitfalls. *Eur J Neurol*. <https://doi.org/10.1111/ene.15443>
93. Bede P, Murad A, Hardiman O (2021) Pathological neural networks and artificial neural networks in ALS: diagnostic classification based on pathognomonic neuroimaging features. *J Neurol*. <https://doi.org/10.1007/s00415-021-10801-5>
94. Bede P, Murad A, Lope J, Li Hi Shing S, Finegan E, Chipika RH, Hardiman O, Chang KM (2021) Phenotypic categorisation of individual subjects with motor neuron disease based on radiological disease burden patterns: a machine-learning approach. *J Neurol Sci* 432:120079. <https://doi.org/10.1016/j.jns.2021.120079>
95. Bede P, Pradat PF, Lope J, Vourc'h P, Blasco H, Corcia P (2022) Primary lateral sclerosis: clinical, radiological and molecular features. *Rev neurol* 178(3):196–205. <https://doi.org/10.1016/j.neurol.2021.04.008>
96. Feron M, Couillandre A, Mseddi E, Termoz N, Abidi M, Bardinet E, Delgadillo D, Lenglet T, Querin G, Welter ML, Le Forestier N, Salachas F, Bruneteau G, Del Mar AM, Debs R, Lacomblez L, Meininger V, Pelegrini-Issac M, Bede P, Pradat PF, de Marco G (2018) Extraparamidal deficits in ALS: a combined biomechanical and neuroimaging study. *J Neurol* 265(9):2125–2136. <https://doi.org/10.1007/s00415-018-8964-y>